







Mechano-electrical interactions and heterogeneities in wild-type and drug-induced long QT syndrome rabbits

Raphaella D. Lewetag^{1,2} , Saranda Nimani³, Nicolò Alerni³, Tibor Hornyik^{1,2,3}, Simon F. Jacobi^{2,4}, Robin Moss^{2,5}, Marius Menza⁶, Nicolas Pilia⁷, Teo P. Walz^{2,5} , Amir HajiRassouliha⁸, Stefanie Perez-Feliz², Manfred Zehender¹, Gunnar Seemann² , Callum M. Zgierski-Johnston² , Ruben Lopez³  and Katja E. Odening^{1,3} 

¹Department of Cardiology and Angiology I, University Heart Center Freiburg, University Medical Center Freiburg, Freiburg, Germany

²Institute for Experimental Cardiovascular Medicine, University Heart Center Freiburg – Bad Krozingen and Faculty of Medicine, University of Freiburg, Freiburg, Germany

³Translational Cardiology, Department of Cardiology and Department of Physiology, University Hospital Bern, Bern, Switzerland

⁴Department of Congenital Heart Defects and Pediatric Cardiology, University Heart Center Freiburg, Faculty of Medicine, University of Freiburg, Freiburg, Germany

⁵Fraunhofer Institute for High-Speed Dynamics, Ernst-Mach-Institute EMI, Freiburg, Germany

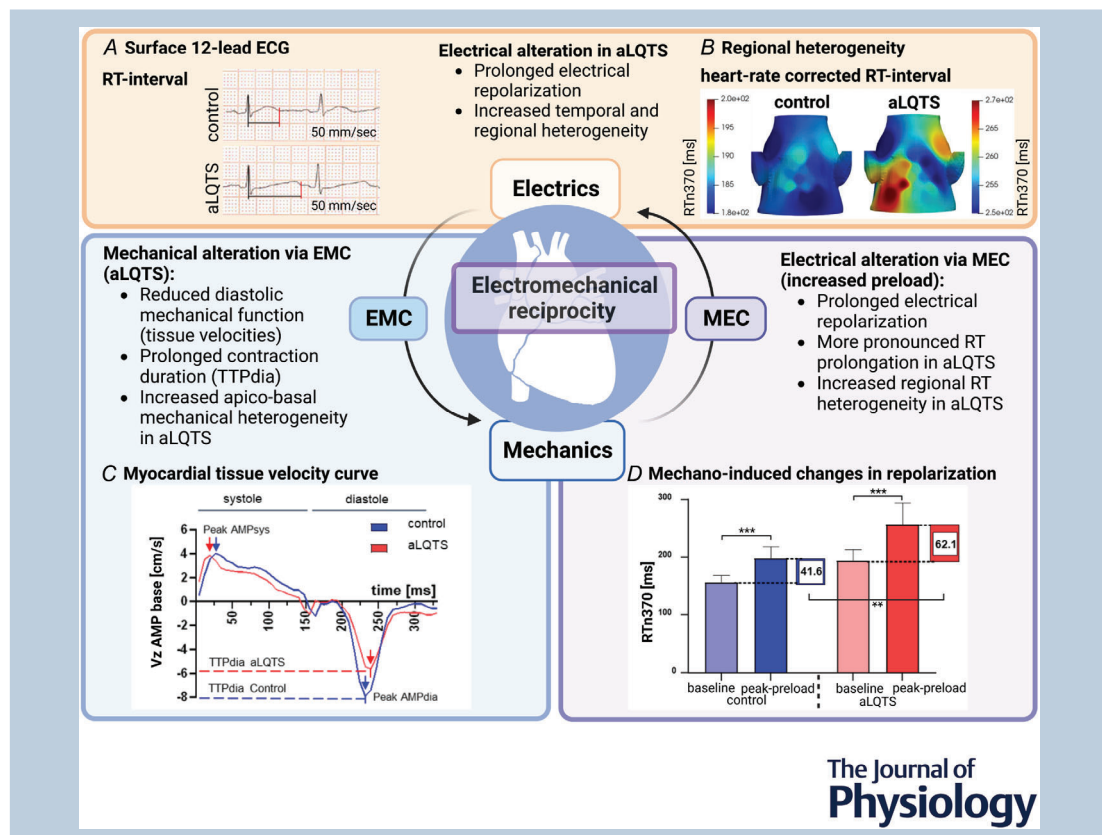
⁶Department of Radiology, Medical Physics, University Hospital Freiburg, and Faculty of Medicine, University of Freiburg, Germany

⁷Karlsruhe Institute of Technology, Karlsruhe, Germany

⁸Auckland Bioengineering Institute, Auckland, New Zealand

Handling Editors: Peter Kohl & Eilidh MacDonald

The peer review history is available in the Supporting information section of this article (<https://doi.org/10.1113/JP284604#support-information-section>).



R. D. Lewetag, S. Nimani and N. Alerni contributed equally as co-first authors.

Abstract Electromechanical reciprocity – comprising electro-mechanical (EMC) and mechano-electric coupling (MEC) – provides cardiac adaptation to changing physiological demands. Understanding electromechanical reciprocity and its impact on function and heterogeneity in pathological conditions – such as (drug-induced) acquired long QT syndrome (aLQTS) – might lead to novel insights in arrhythmogenesis. Our aim is to investigate how electrical changes impact on mechanical function (EMC) and vice versa (MEC) under physiological conditions and in aLQTS. To measure regional differences in EMC and MEC *in vivo*, we used tissue phase mapping cardiac MRI and a 24-lead ECG vest in healthy (control) and I_{K_r} -blocker E-4031-induced aLQTS rabbit hearts. MEC was studied *in vivo* by acutely increasing cardiac preload, and *ex vivo* by using voltage optical mapping (OM) in beating hearts at different preloads. In aLQTS, electrical repolarization (heart rate corrected RT-interval, RTn370) was prolonged compared to control ($P < 0.0001$) with increased spatial and temporal RT heterogeneity ($P < 0.01$). Changing electrical function (in aLQTS) resulted in significantly reduced diastolic mechanical function and prolonged contraction duration (EMC), causing increased apico-basal mechanical heterogeneity. Increased preload acutely prolonged RTn370 in both control and aLQTS hearts (MEC). This effect was more pronounced in aLQTS ($P < 0.0001$). Additionally, regional RT-dispersion increased in aLQTS. Motion-correction allowed us to determine APD-prolongation in beating aLQTS hearts, but limited motion correction accuracy upon preload-changes prevented a clear analysis of MEC *ex vivo*. Mechano-induced RT-prolongation and increased heterogeneity were more pronounced in aLQTS than in healthy hearts. Acute MEC effects may play an additional role in LQT-related arrhythmogenesis, warranting further mechanistic investigations.

(Received 27 February 2023; accepted after revision 18 April 2023; first published online 20 April 2023)

Corresponding author K. E. Odening: Department of Physiology and Department of Cardiology, University Bern and University Hospital Bern, Buehlplatz 5, CH-3012 Bern, Switzerland. Email: katja.odening@unibe.ch and katja.odening@insel.ch

Abstract figure legend Electromechanical reciprocity in healthy (control) and acquired long QT syndrome (aLQTS) rabbit hearts. *A* and *B*, electrical alteration in aLQTS. *A*, exemplary ECG traces demonstrating I_{K_r} -blocker E-4031-induced RT prolongation in aLQTS. *B*, visualisation of heart rate corrected RTn370 (each colour-coded scale includes 20 ms) on rabbits' torso in aLQTS compared to control ($n = 6$ each). *C*, electro-mechanical coupling (EMC). Exemplary myocardial longitudinal velocity curve in base (cm/s) during cardiac cycle in control (blue) and aLQTS (red). Indicated are peak amplitudes (AMPsys, AMPdia) and time-to-diastolic peak (TTPdia). *D*, mechano-electrical coupling (MEC). Box plots of preload induced changes in repolarization. Comparison between the time points *baseline* (15 s before increase in preload) and time of the maximal RTn370 increase *peak-preload* (around 20 s after NaCl bolus injection). Heart rate corrected RTn370 demonstrates more pronounced RT-changes in aLQTS compared to control ($n = 13$ each).

Key points

- Electromechanical reciprocity comprising excitation-contraction coupling (EMC) and mechano-electric feedback loops (MEC) is essential for physiological cardiac function.
- Alterations in electrical and/or mechanical heterogeneity are known to have potentially pro-arrhythmic effects.
- In this study, we aimed to investigate how electrical changes impact on the mechanical function (EMC) and vice versa (MEC) both under physiological conditions (control) and in acquired long QT syndrome (aLQTS).
- We show that changing the electrical function (in aLQTS) results in significantly altered mechanical heterogeneity via EMC and, vice versa, that increasing the preload acutely prolongs repolarization duration and increases electrical heterogeneity, particularly in aLQTS as compared to control.

- Our results substantiate the hypothesis that LQTS is an ‘electro-mechanical’, rather than a ‘purely electrical’, disease and suggest that acute MEC effects may play an additional role in LQT-related arrhythmogenesis.

Introduction

Electrical and mechanical heterogeneity are an important prerequisite for physiological cardiac function (Janse et al., 2012; Solovyova et al., 2016). Driven by regional heterogeneities in the expression of cardiac ion channels, electro-mechanical heterogeneity exists between right and left ventricles (RV, LV), in apico-basal and transmural directions (Antzelevitch & Fish, 2001; Janse et al., 2012; Solovyova et al., 2016). Acute or chronic changes in electrical function can alter mechanical function and vice versa, via electro-mechanical (EMC) and mechano-electric (MEC) coupling (Quinn & Kohl, 2021). Recently denominated as ‘electromechanical reciprocity’ (Odening et al., 2022), it is responsible for alterations in both global and local electro-mechanical function (leading to heterogeneity). A variety of different stretch-activated or stretch-sensitive channels have been identified as mediators of MEC (Quinn & Kohl, 2021).

Electromechanical reciprocity is not only present in healthy hearts, but can also be observed and accentuated in ‘electrical’ heart diseases such as long QT syndrome (LQTS), in which cardiac repolarization and the QT interval are prolonged and patients are prone to ventricular tachycardia, arrhythmic syncope and sudden cardiac death (Roden, 2008). LQTS can either be inherited due to mutations in genes encoding for cardiac ion channels (Schwartz et al., 2012) or – more frequently – acquired (Roden, 2004) as a result of drugs that impair cardiac ion channel function. Recent experimental and clinical data suggest that LQTS hearts not only demonstrate electrical abnormalities but also exhibit mechanical dysfunction (altered diastolic relaxation and prolonged contraction duration), altered mechanical heterogeneity and impaired electromechanical interaction (electromechanical window), which correlate with the individual’s risk for arrhythmia development (Haugaa, Edvardsen, et al., 2009; Haugaa, Amlie, et al., 2010; Lang, Koren et al., 2016; Nador et al., 1991; Odening et al., 2013), and are

likely linked to LQT-related arrhythmogenesis (Odening et al., 2022).

In this project, we aimed at characterising EMC and MEC in rabbits *in vivo* and *ex vivo* in the healthy state and in acquired LQTS (aLQTS).

We chose the rabbit as it mimics human cardiac physiology more closely than smaller lab animals: Rabbit and human hearts share pronounced similarities in ion currents and the shape of action potentials (Nerbonne, 2000), regional systolic and diastolic behaviour (Jung et al., 2012) and in MEC mechanisms (Quinn & Kohl, 2016). To exclude a potential impact of chronic electro-mechanical remodelling in inherited LQTS, we utilised an acute, drug-induced LQTS model using the I_{Kr} -blocker E-4031.

Methods

Ethical approval

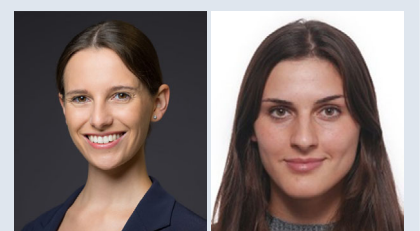
All animal experiments were performed in accordance with EU legislation (directive 2010/63/EU) and the German and Swiss animal welfare laws (TierSchG and TierSchVersV), after approval by the animal welfare committee of the local authorities (Regierungspräsidium Freiburg; approval number G18-118; Kanton Bern, Amt für Veterinärwesen, approval number BE115/2019). We confirm that all animal experiments in this study correspond to *The Journal’s* animal ethics checklist as outlined in the instructions to the authors.

Animal studies

Adult male and female *New Zealand White* rabbits of similar age and weight were used and obtained from our own breeding at University Hospital Freiburg and from Charles River Laboratories, France. The feeding regime took place *ad libitum*.

For anaesthesia, a bolus of 0.5 ml/kg body weight (BW) ketamine S (Ketanest S 25 mg/ml, Pfizer, New York,

Raphaela D. Lewetag completed her medical studies and is currently finishing her Dr med. thesis in the Department of Cardiology and Angiology I at the University of Freiburg, Germany. Her research focuses on cardiac electromechanical reciprocity under physiological conditions and in pathological acquired long-QT syndrome. **Saranda Nimani** is a medical doctor and is currently doing her PhD research in the Translational Cardiology/Electrophysiology Group at the University of Bern, Switzerland. Her research focuses on arrhythmogenic mechanisms and novel therapeutic approaches in genetic arrhythmia disorders, short-QT and long-QT syndrome.



USA) and 0.2 ml/kg/BW xylazine (Rompun 2%, Bayer, Leverkusen, Germany) was administered intra-muscularly (i.m.). This was followed by continuous intravenous (i.v.) infusion of 1–6 ml/h ketamine S/xylazine (titrated by anaesthesia-depth) during 12-lead ECG, 24-lead vest ECG and tissue phase mapping cardiac MRI *in vivo*, since this combination does not affect cardiac repolarization (Odening et al., 2008). The depth of anaesthesia was determined by measuring heart and respiratory rate. *Ex vivo* beating heart excision for optical mapping (OM) was performed in anaesthetised rabbits after additional injection of 500 IU heparin i.v. (heparin-sodium, 25,000 IU/ml, Braun, Melsungen, Germany) and humane killing with 40 mg/kg BW thiopental i.v. (Thiopental-sodium 0.5 g, Inresa, Freiburg, Germany), according to the German and Swiss animal welfare laws and *The Journal's* humane killing standards.

12-lead ECG

In vivo conventional 12-lead surface ECGs were performed in rabbits anaesthetised with ketamine S/xylazine as described above ($n = 13$ per group). ECGs were recorded in each rabbit under physiological conditions (control) followed by measurement with I_{Kr} -blocker E-4031 (aLQTS; 10 μ g/kg BW bolus; continuous 1 μ g/kg BW/min infusion i.v.). ECGs were performed in both groups – control and aLQTS – at *baseline* and *peak-preload* time points (20 s after the injection of 6 ml/kg BW 0.9% NaCl bolus i.v., heated up to body temperature). Instead of conventional QT-interval, RT-intervals were measured to be in line with automated RT-interval annotations in the 24-lead ECG vest (see below). RT-intervals were adjusted to heart beating frequency via calculation of heart rate corrected RTn370 (using $RTn370 = RT_{observed} - (0.22 \times (RR_{observed} - 370))(\text{ms})$) (Brunner et al., 2008; Ziupa et al., 2019). Temporal heterogeneity of repolarization was parameterised by the short-term variability of RT ($STV_{RT}(\text{ms}) = \sum_{n=1}^N \frac{|RT_{n+1} - RT_n|}{(N)^2}$, assessed in 31 consecutive beats) (Baumert et al., 2016). Regional heterogeneity of repolarization was parameterised by RT-dispersion (max-min) ($RTn370 = RT_{observed} - (0.22 \times (RR_{observed} - 370))(\text{ms})$, assessed in six consecutive beats over 12 leads).

12-lead ECG with pharmacological autonomic blockade

To determine whether the observed mechano-induced electrical changes are (mainly) driven by cardiac-intrinsic mechanisms and not secondary by autonomic reflexes, the same experiments were performed with pharmacological autonomic blockade ($n = 8$ per group). For the

pharmacological blockade of sympathetic reflexes, an i.v. bolus of 0.5 ml/kg BW esmolol (Esmolol OrPha, 2 mg/ml) was administered in rabbits anaesthetised as described above, followed by continuous i.v. infusion of 1.5 ml/kg/h esmolol. For the pharmacological blockade of parasympathetic reflexes, an i.m. injection of 0.1 ml/kg glycopyrronium bromide (Robinul 0.1 mg/ml) was administered. Both dosages correspond to the recommendations of the VetPharm website for a complete autonomic blockade (www.vetpharm.uzh.ch).

ECGs were recorded continuously at baseline and after bolus injection (20 s after the injection of 6 ml/kg BW 0.9% NaCl bolus i.v., heated up to body temperature) and the *baseline* and *peak-preload* time points with and without blocker administration were compared. Measurements were performed at 2 days (day 1 with blockers, and day 2 without blockers), ensuring the time points of measurements matched between conditions.

24-lead ECG vest

Body surface potentials were recorded using a self-fabricated vest in combination with a 24-lead EEG active-electrode ActiveTwo system (BioSemi B.V., Amsterdam, The Netherlands) (Moss et al., 2022). The electrode placement in the vest in relation to the heart position can be seen in Fig. 2F and G and was extracted from previous CT imaging data as described in Moss et al. (2022). Figure 2H shows the automated signal annotation of R-peak and T-end that was performed in collaboration with the Karlsruhe Institute of Technology (KIT), Institute of Biomedical Engineering using the open-source *ECGdeli toolbox for MATLAB* (Pilia et al., 2021) (MATLAB R2019a, The MathWorks, Inc.). 24-lead vest ECGs (vECG) were performed *in vivo* in anaesthetised rabbits ($n = 6$ per group). Recordings were performed at two time points, *baseline* and *peak-preload* (20 s after the injection of 6 ml/kg BW 0.9% NaCl bolus i.v., heated up to body temperature) in each rabbit under physiological conditions (control) and during E-4031-infusion (aLQTS) (see above). RR-interval, RT-duration, heart rate corrected RTn370-duration and STV_{RT} were assessed. The regional variation of RT-interval was calculated using the following equation: $RT_{\text{difference}}(i) [\text{ms}] = RTn360(i) - \min_{I(1 \rightarrow 24)} RTn360(i)$, with i being the examined lead and I being the lead with the shortest RT-interval. This enabled the visualisation of regional differences in repolarization across the rabbits' torso (Fig. 2I and J).

Tissue phase mapping (TPM-MRI)

To assess regional myocardial longitudinal (V_z) and radial tissue velocities (V_r), rabbits anaesthetised with ketamine S/xylazine (as described above, $n = 19$ per

group) were subjected to TPM-MRI in a 1.5T MR machine (Avanto, Siemens, Germany) with high temporal (7.6 ms) and spatial resolution ($1.0 \times 1.2 \times 4$ mm) (further described in Jung et al., 2012; Odening et al., 2013). Systolic and diastolic velocities were acquired in each rabbit under physiological conditions (control) and during E-4031 infusion (aLQTS) (see above). Systolic and diastolic peak velocities (AMPsys and AMPdia, respectively) as well as *time-to-diastolic peak* duration (TTPdia), a marker for contraction duration (Odening et al., 2013; Ziupa et al., 2019), were derived from left ventricular (LV) tissue velocity curves in both longitudinal (Vz) and radial (Vr) directions (Fig. 3A–D). To this end, the LV was partitioned into 16 segments in the base, mid and apex (modified American Heart Association model) (Cerqueira et al., 2002). As *time-to-diastolic peak* duration is heart rate dependent, but an accurate heart rate correction formula has not yet been defined, we measured and compared *time-to-diastolic peak* only in rabbits with similar RR-interval duration in control and aLQTS measurements ($n = 9$). Data processing was accomplished by using customised MATLAB software.

Langendorff-perfusion of rabbit hearts

Rabbits were anaesthetised with ketamine S/xylazine (12.5/3.75 mg/kg) i.m. and were administered 1000 IU heparin i.v. via ear vein injection ($n = 6$). Following humane killing with thiopental-sodium i.v. (40 mg/kg BW), the heart was rapidly excised, and cannulated on a modified Langendorff perfusion system (Hugo Sachs). The heart was perfused with a modified Krebs–Henseleit (KH) solution at constant pressure (80 mmHg) (Hornyk et al., 2020). Aortic pressure, flow rate, and temperature were monitored and a pseudo-ECG (monopolar Ag/AgCl pellet electrodes in the solution near the cardiac surface) was recorded.

A modified version of the Langendorff-perfused heart set-up was used to study MEC *ex vivo*. In this ‘working-heart-like’ configuration, a latex balloon was placed into the LV and was used to set different end-diastolic LV pressure levels to mimic different preloads. The balloon was filled with KH solution and was connected via tubes to a water column (in a calibrated cylinder). The calibrated cylinder was positioned at different heights relative to the heart, thereby providing the desired preload levels (0, 6, 15 mmHg), while enabling ‘free’ contraction of the LV (hence the term: ‘working-heart-like’ configuration).

Panoramic optical mapping of beating hearts

A combined Langendorff and OM setup was used to study regional heterogeneities in electrical (action potential) characteristics and mechano-electrical inter-

actions *ex vivo* (Fig. 1). A three-view mirror-based panoramic OM system was used with healthy and aLQTS hearts ($n = 6$ per group). Acquired LQTS was obtained by adding 50 nM E-4031 into the KH solution to inhibit I_{Kr} -channels after the baseline measurements, and perfusion was maintained for at least 10 min before action potential duration (APD) measurements were started. Voltage-sensitive dye (Di-4-ANBDQPQ, Cytochrome, Buffalo, NY, USA) was injected directly into the aortic root for coronary perfusion (20 μ l of 8.6 mM injected in 0.5 μ l increments over 5 min). The hearts were paced at 2.5 Hz with an electrical stimulator on the left atrium to maintain a normal ventricular activation via an intact conduction system. In contrast to the standard OM approach, no pharmacological motion uncoupler agent (e.g. blebbistatin) was applied to maintain normal mechanical contraction. The three cardiac views were projected with mirrors onto one sCMOS camera (Andor Zyla 5.5, Oxford Instruments, UK) recording at a frame rate of 200 Hz. Multiple red light-emitting diodes (LED CBT-90-RX/B, Luminus Devices, Inc. Sunnyvale, CA, USA; filter: ZET642/20X; Chroma) were used for excitation. Fluorescence emission was collected via a high-speed lens (DO-5095, Navitar) and a custom emission filter (ET585/50M+800/200M, Chroma).

MEC was studied both in healthy and aLQTS hearts by detecting changes in electrical characteristics (ECG and action potential parameters) following rapid alterations in mechanical function by changing LV preload (preloads: 6–0–15–6 mmHg). For analysis of fluorescence signals, the acquired files were cropped to ensure that each recording starts at diastole and the recordings were averaged across multiple heart beats to obtain an optical recording of a single action potential with a high signal-to-noise ratio.

Following beat averaging, motion correction of the resulting OM signals was used to separate motion-induced and voltage-induced changes in fluorescence of the beating hearts. A published sub-pixel image registration approach was used to track changes between an image of the heart in diastole (base image) and during contraction (HajiRassouliha et al., 2017, 2018). Sub-image sizes of 32 pixels were used with step sizes of 20 pixels (CC32SS20) to find the tracked points between images. These were used to predict the location of each pixel from the base image on each of the tracked images. The intensity value at each of these locations was then estimated by interpolating between pixels in the image being motion corrected. The resulting intensities formed the motion corrected image. Subsequently, the data were analysed with a custom-made MATLAB (Mathworks) program for OM analysis (available from the authors on request). For this purpose, the signals were normalised and inverted, and regions of interest (ROIs) 10×10 pixel

(2.6×2.6 mm) in size were defined as follows: LV base (ROI 1), mid (ROI 2), and apex – anterior view; RV base (ROI 3) and LV base (ROI 4) – left-posterior view; RV mid (ROI 5) – right-lateral view.

Statistical analysis

Statistical analysis was performed using GraphPad Prism 8 (GraphPad Software, San Diego, USA). Data are expressed as means \pm standard deviation. Comparison of control and aLQTS rabbits was performed using paired Student's *t* test, and significance was established at $P < 0.05$. The *n* value reflects the number of rabbits used per group (e.g. $n = 13$ per group, that is 13 control and 13 aLQTS animals).

Results

Alteration of cardiac repolarization in acquired LQTS *in vivo*

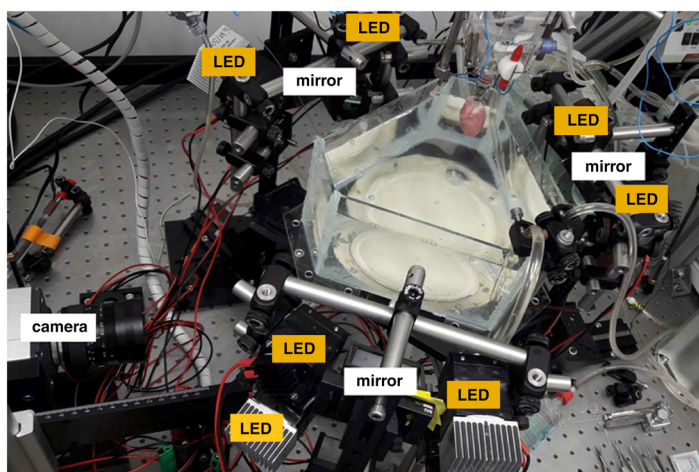
Prolongation of heart rate corrected RT-interval. 12-lead surface ECG (Fig. 2A) demonstrated a prolongation of cardiac repolarization during the infusion of I_{Kr} -blocker E-4031 (aLQTS) in all individual animals (Fig. 2B). The RT-interval prolonged (control 163.85 ± 18.54 ms vs. aLQTS 194.69 ± 25.34 ms, $P < 0.0001$, $n = 13$ per group), while the RR-intervals slightly decreased (e.g. heart rates increased) (control 402.39 ± 55.56 ms vs. aLQTS 373.23 ± 47.00 ms, $P = 0.021$, $n = 13$ per group), leading to a pronounced prolongation of heart rate corrected RTn370-interval in aLQTS (control 156.61 ± 11.59 ms vs.

aLQTS 193.95 ± 19.60 ms, $P < 0.0001$, $n = 13$ per group) (Fig. 2B).

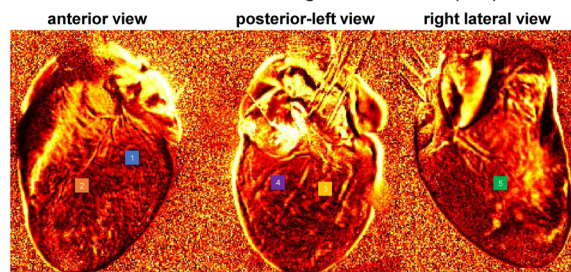
Increased temporal and regional heterogeneity of repolarization. To elucidate ECG parameters indicative of an increased pro-arrhythmic risk in aLQTS, temporal and regional heterogeneity of repolarization were assessed. Short-term variability of RT (STV_{RT}) – a marker for temporal heterogeneity of repolarization – was significantly increased in aLQTS compared to control (Fig. 2C). Similarly, RT-dispersion (max-min) – a marker for regional heterogeneity of repolarization – was increased significantly during the infusion with I_{Kr} -blocker E4031 (Fig. 2D).

The calculation of the deviation of the individual RT from the shortest RT in the vECG enabled a visualisation of the regional variation of RT-interval ($RT_{\text{difference}}$) projected on the rabbits' thoraces. While in the LV basal region no remarkable differences were apparent in the pattern of regional RT-interval variation between both groups, RTn370 increased in the apical region in aLQTS compared to control, with a significant increase in $RT_{\text{difference}}$ in lead 21 and 22 (as indicated by the higher colour-gradient; lead 21, $P = 0.004$, lead 22, $P = 0.041$, $n = 5$ per group) (Fig. 2I and J). Moreover, in aLQTS the change in regional RT-interval was visually noticeable in the leads depicting the RV (leads 10, 15, 17, 23) with particularly pronounced changes in $RT_{\text{difference}}$ (indicated in red in Fig. 2I and J) in 4 out of 6 animals. In these, the RV-LV difference was 3.46 ± 1.73 ms in control and increased to 9.09 ± 5.28 ms in aLQTS ($P = 0.13$, paired *t* test, Fig. 2E, I and J).

A Setup for panoramic optical mapping of beating Langendorff-perfused heart



B Different views and selected regions of interest (ROI)



C Representative AP tracings before and after motion correction

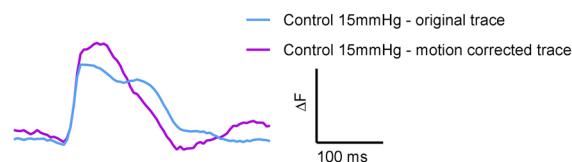


Figure 1. Optical mapping setup and examples of motion correction

A, image of the panoramic optical mapping setup. Indicated are LEDs, mirrors and the camera position. B, illustration of the three different views of the heart (anterior, left-posterior, and right-lateral) and corresponding selected regions of interest (ROIs). C, exemplary fluorescence tracings before and after motion correction. ΔF = change in fluorescence intensity in arbitrary units.

Induction of mechanical alterations via EMC *in vivo*

Using tissue-phase mapping MRI, which allows a detailed analysis of regional cardiac function, the effect of electrical changes (e.g. prolongation of cardiac repolarization in aLQTS) on mechanical features was assessed.

Myocardial systolic and diastolic velocities. Peak systolic (AMPsys) and diastolic (AMPdia) tissue velocities in radial (Vr) and longitudinal (Vz) directions were compared between control and aLQTS. In line with a prolongation of cardiac repolarization, E-4031 infusion increased systolic peak velocities in 1 out of 16 longitudinal (Vz AMPsys, $n = 19$ per group) and 5 out of 16 radial (Vr AMPsys, $n = 19$ per group) LV segments,

indicating an improved systolic function (Table 1). While radial diastolic peak velocities (Vr AMPdia) remained unchanged, longitudinal diastolic peak velocities (Vz AMPdia) were significantly decreased in 6/6 basal and 4/6 mid segments in aLQTS compared to control (Fig. 3B), suggesting an E-4031-induced diastolic dysfunction via EMC.

Time-to-diastolic peak. Time-to-diastolic peak duration, a marker for the duration of contraction and early relaxation, was significantly prolonged in 9/16 segments in the longitudinal (Vz, Fig. 3C) and 3/16 segments in radial (Vr, Table 2) of the rabbits' LV in aLQTS compared to control.

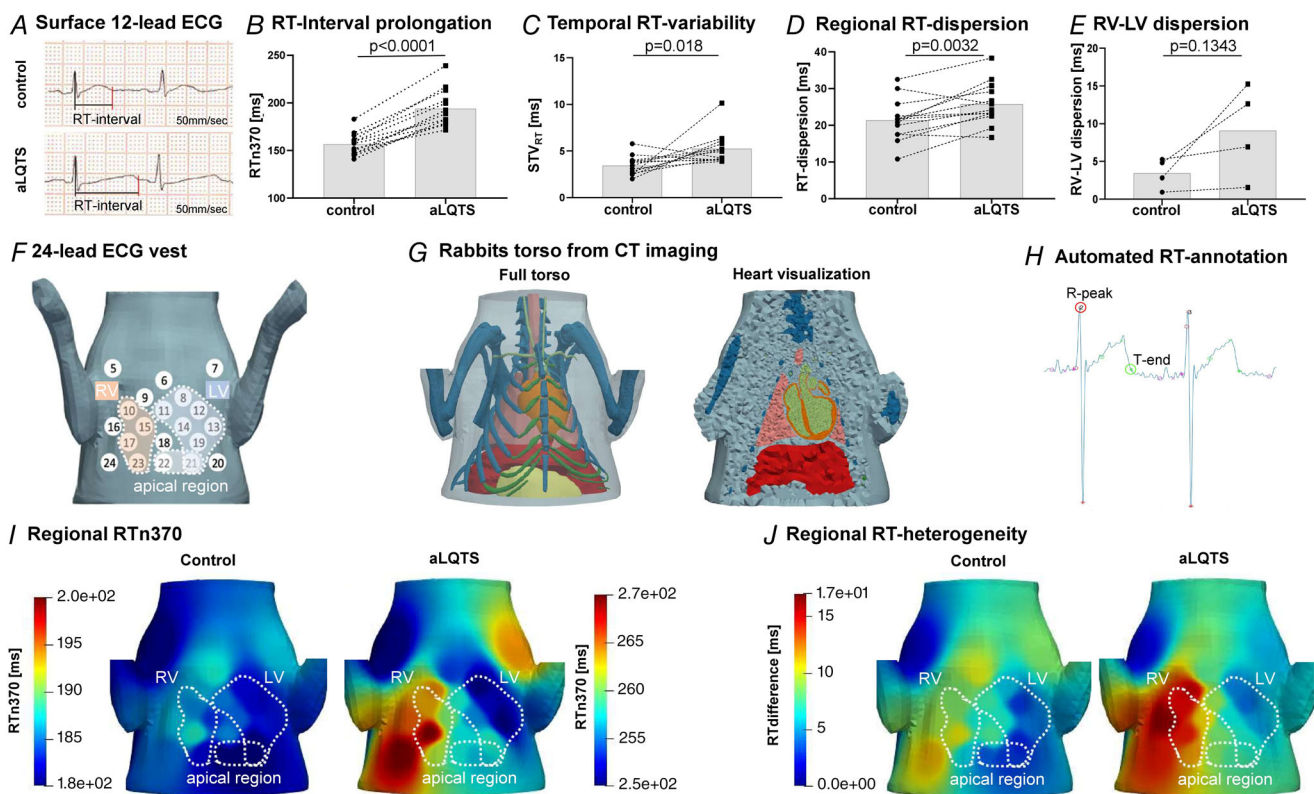


Figure 2. Electrical alterations in acquired LQTS (induced by I_{Kr} -blocker E-4031)

A–D, 12-lead surface ECG. E–J, 24-lead ECG vest. A, example ECG traces demonstrating E-4031-induced RT prolongation in aLQTS. B, dot plots graph indicating prolongation of RR-adjusted RTn370-interval in all individual rabbits after E-4031 administration compared to control ($n = 12$ each). C, dot plots graph indicating increased temporal RT-variability (short-term variability of RT, STV_{RT}) in aLQTS compared to control ($n = 13$ each). D, dot plots graph demonstrating increased regional RT-dispersion (RT-dispersion (max-min)) in aLQTS compared to control ($n = 13$). E, dot plots graph demonstrating increased RV-LV dispersion (ms) in aLQTS compared to control ($n = 4$). F, schematic illustration of arrangement of ECG-leads on the ventral side of the 24-lead ECG vest (lead 5–24). G, CT-based modelling of the rabbits' torso and organs (left; dark-blue: bones, dark-green: cartilage, orange: heart, salmon: lungs, brown: liver; light-green: blood, yellow: stomach) and visualisation of a transversal cut through the meshed geometry of the torso (right). H, example illustration of automated ECG vest signal-annotation. I, visualisation of RTn370 (each colour-coded scale includes 20 ms) on rabbits' torso in aLQTS compared to control ($n = 6$ each). J, visualisation of regional RT-heterogeneity (colour-coded as differences compared to minimum RT) on rabbits' torso in aLQTS compared to control ($n = 6$ each). F and G modified from (Moss et al., 2022) with permission.

Table 1. E-4031 induced changes in systolic tissue velocity (Vz AMPsys, Vr AMPsys)

		Control (n = 19)		aLQTS (n = 19)		Student's <i>t</i> test
Vz AMPsys (cm/s)		Mean	SD	Mean	SD	
Apex	Septal	1.83	1.11	2.53	1.33	<i>P</i> = 0.0042
Vr AMPsys (cm/s)						
Mid	Anterior	1.78	0.27	2.02	0.48	<i>P</i> = 0.0224
	Anterolateral	1.67	0.34	1.90	0.44	<i>P</i> = 0.0186
Apex	Anterior	1.23	0.29	1.50	0.38	<i>P</i> = 0.0223
	Lateral	1.27	0.39	1.55	0.40	<i>P</i> = 0.0233
	Septal	1.34	0.25	1.69	0.55	<i>P</i> = 0.0051

Table 2. E-4031 induced changes in radial diastolic contraction duration (Vr TTPdia)

		Control (n = 9)		aLQTS (n = 9)		Student's <i>t</i> test
Vr TTPdia (ms)		Mean	SD	Mean	SD	
Base	Anterolateral	220.82	30.43	229.27	39.49	<i>P</i> = 0.0208
	Inferolateral	210.69	26.54	229.27	35.44	<i>P</i> = 0.0286
Mid	Inferior	234.33	22.80	247.84	26.72	<i>P</i> = 0.0145

Apico-basal heterogeneity in mechanical function. To investigate the impact of the increased repolarization heterogeneity in aLQTS on regional mechanical heterogeneity, we calculated apico-basal heterogeneity, defined as difference between all basal and all apical values. In aLQTS, apico-basal heterogeneity in longitudinal diastolic peak velocities (Vz AMPdia) showed a significant decrease compared to control (control -4.34 ± 1.19 cm/s vs. aLQTS -3.18 ± 1.19 cm/s, *P* = 0.0008, *n* = 17 per group) (Fig. 3E). In contrast, apico-basal heterogeneity in longitudinal *time-to-diastolic peak* duration (Vz TTPdia) was significantly increased in aLQTS compared to control (control 4.16 ± 8.82 ms vs. aLQTS 20.54 ± 10.31 ms, *P* = 0.037, *n* = 8 per group) (Fig. 3F), indicating an impact of electrical changes also on mechanical heterogeneity.

Mechano-induced changes in electrical (dys-)function via MEC *in vivo*

In surface ECG-measurements, alterations in mechanical function (via increased preload) resulted in changes of electrical function via MEC.

Mechano-induced changes in RR and RT intervals. RT-intervals were prolonged and heart rate increased (i.e. RR-intervals shortened) after acute 0.9% NaCl i.v. bolus application under physiological conditions (control) and with I_{Kr} -blocker E-4031 (aLQTS) (Fig. 4A). Heart rate changes did not differ significantly between control

and aLQTS groups. Heart rate corrected RTn370-intervals were prolonged in both groups (Fig. 4Bb). Interestingly, RTn370 prolongation was significantly more pronounced in aLQTS compared to control (*P* = 0.0056, *n* = 13 per group) (Fig. 4Bb), indicating that cardiac repolarization in aLQTS may be more susceptible to acute MEC effects than in healthy (control) hearts.

Arterial blood pressure was measured in both groups at *baseline* (15 s before increase in preload) and at the time of the maximal RTn370 increase (around 20 s after NaCl bolus injection) in *n* = 5 rabbits. Mean arterial blood pressure (MAP) decreased significantly in both groups following bolus injection (in the range of 6–8 mmHg) (Fig. 5Aa). Importantly, the delta between *baseline* and *RTn370-peak* ($\Delta_{peak-baseline}$) showed no significant difference between control and aLQTS (Fig. 5Ab).

To further investigate whether the observed changes in the electrical function (RT) are mainly due to intrinsic mechano-induced electrical changes or whether (some parts of it) are mediated secondarily by autonomic reflexes, we performed additional experiments in a subset of control rabbits before and after complete blockade of the parasympathetic and sympathetic system. Heart rate measurements were performed to validate the pharmacological autonomic blockade. While no changes in heart rate were observed due to betablockade alone, probably due to parasympathetic predominance in rabbits anaesthetised with xylazine and the consecutive slow heart rate, we observed an increase in heart rate after the parasympathetic blocker was also added (Fig. 5Bc). In these experiments, the bolus-induced changes in RTn370

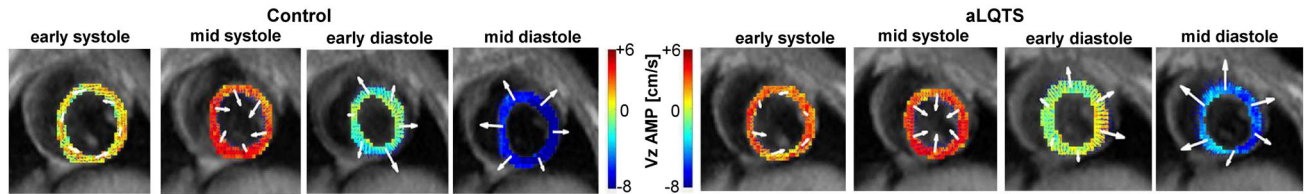
did not differ between baseline and autonomic-blockade experiments (Fig. 5B), suggesting a direct role of myocardial stretch caused by increased preload on the observed electrical alterations.

Mechano-induced changes in heterogeneity of repolarization. In 12-lead surface ECG, the increase in preload under physiological conditions (control) resulted in a significant increase in temporal heterogeneity, so called STV_{RT} , as seen in Fig. 4C. In aLQTS, in which the *baseline* STV_{RT} was already pronouncedly higher than in controls, there was no significant increase in

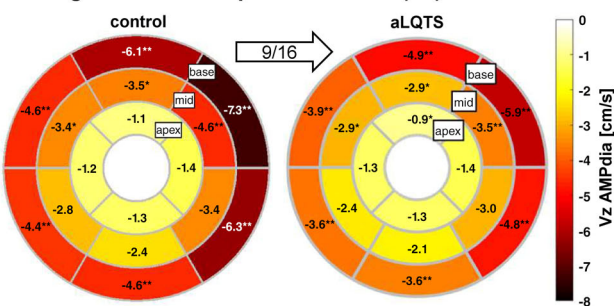
STV_{RT} from *baseline* to *peak-preload* (Table 3). Regional RT-dispersion (max-min) from baseline to peak was only increased significantly in aLQTS and showed no significant change in healthy rabbit hearts (Table 3).

The pattern in regional RT-heterogeneity obtained from the 24-lead ECG vest recordings in $n = 6$ rabbits per group changed with increased preload. Regional variation of the individual RT from the shortest RT ($RT_{\text{difference}}$) in healthy control revealed only slight changes in leads 10, 15–17 and 23 picturing the RV regions (Fig. 4D), and standard deviation of $RT_{\text{difference}}$ over all 24 leads – depicting regional RT-heterogeneity –

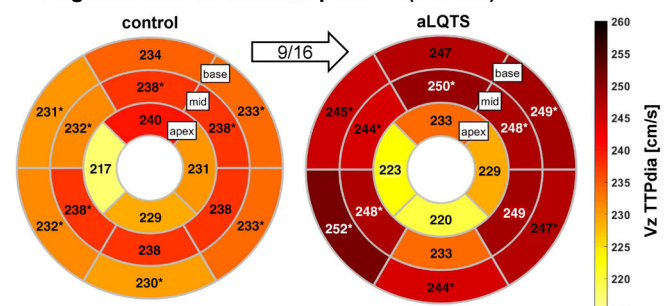
A Regional myocardial velocities during cardiac cycle



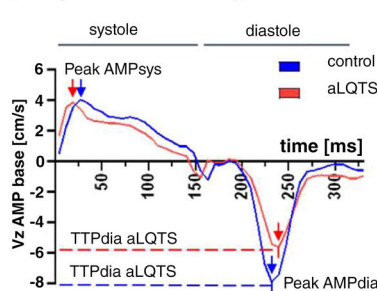
B Regional diastolic peak velocities (Vz)



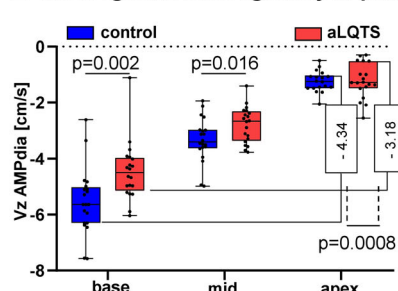
C Regional time-to diastolic peak Vz (TTPdia)



D Myocardial velocity curve



E Interregional heterogeneity in peak Vz



F Interregional heterogeneity in TTPdia

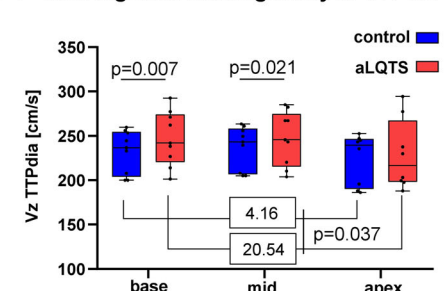


Figure 3. Impact of electrical alterations (aLQTS) on mechanical function (via EMC) in tissue-phase mapping MRI (TPM-MR)

A, example of regional longitudinal velocities (V_z AMP, cm/s, colour-coded as indicated) and radial velocities (indicated by length of arrows) during a cardiac cycle in control and aLQTS. B, bull's eye plots of diastolic peak longitudinal velocities (V_z AMPdia, cm/s) in all basal, mid, and apical segments. Velocities are colour-coded and average values are indicated. Diastolic peak longitudinal velocities decreased in 9 out of 16 segments as indicated in the arrow ($n = 19$ each). C, bull's eye plots of regional time-to-diastolic peak duration in longitudinal velocities (V_z TTPdia, cm/s). V_z TTPdia increased in 9 out of 16 segments as indicated in the arrow ($n = 9$ each). Velocities are colour-coded as indicated. D, example myocardial longitudinal velocity curve in base (V_z AMP, cm/s) during a cardiac cycle in control and aLQTS. E, box plot graph indicating decreased apico-basal heterogeneity in V_z AMPdia in aLQTS compared to control ($n = 19$ each). F, box plot graph indicating increased apico-basal heterogeneity in TTPdia in aLQTS compared to control ($n = 8$ each). * $P < 0.05$, ** $P < 0.01$, *** $P < 0.001$. Detailed mean and SD and exact P values of the TPM-MRI measurements summarised in the bull's eye plots can be found in the statistical summary document.

Table 3. Mechano-induced changes in heterogeneity of repolarization

	Control			aLQTS		
	Baseline (n = 13)	Peak-preload (n = 13)	Student's t test	Baseline (n = 13)	Peak-preload (n = 13)	Student's t test
STV _{RT} (ms)	3.45 ± 1.03	4.84 ± 1.69	P = 0.0254	5.25 ± 1.69	6.09 ± 2.15	n.s. (P = 0.28)
RT-dispersion (max-min) (ms)	21.41 ± 5.73	25.83 ± 5.76	ns (P = 0.13)	25.83 ± 5.76	32.69 ± 12.79	P = 0.0256

Data are presented as means ± SD.

remained almost the same (control *baseline* SD 2.86 ms vs. control *peak* 2.54 ms). In aLQTS, there was no significant change in overall mean RT_{difference} between *baseline* and *peak-preload* (aLQTS *baseline* 8.59 ± 4.25 vs. aLQTS *peak* 9.28 ± 2.78 ms, P = 0.29).

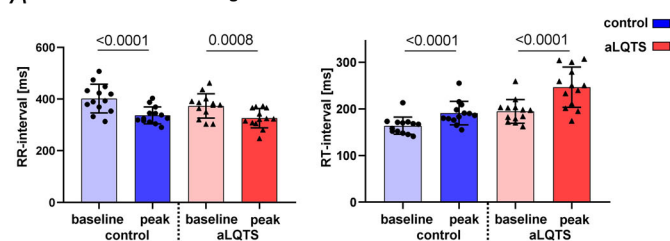
In summary, increased preload-mediated RT-prolongation and RT-heterogeneity altering effects were more pronounced in E-4031-induced aLQTS hearts, indicating that cardiac repolarization in LQTS may be

more susceptible to acute MEC effects than in healthy hearts.

Investigations of MEC *ex vivo* in Langendorff-perfused hearts

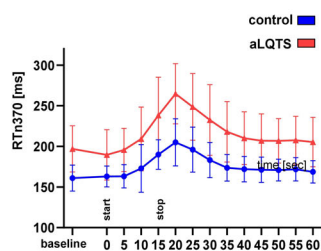
We developed the above-described Langendorff-perfused ‘working-heart-like’ OM setup, with the idea of

A Mechano-induced changes in RR- und uncorrected RT-interval

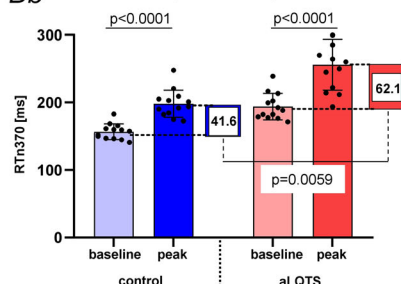


B Increased preload effects on electrical function

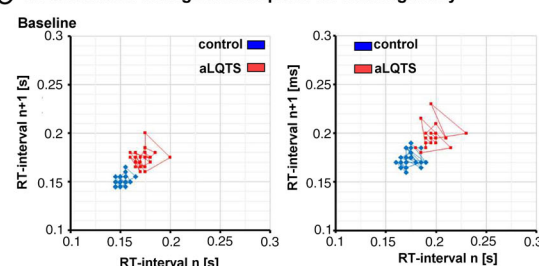
Ba Mechano-induced RTn370 interval changes



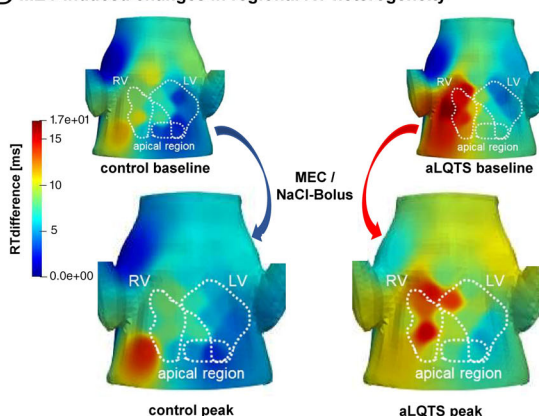
Bb Mechano-induced peak RT changes



C MEC induced changes in temporal RT heterogeneity



D MEC induced changes in regional RT-heterogeneity

**Figure 4. Impact of mechanical alteration (increase in preload) on electrical function (via MEC)**

A and B, 12-lead surface ECG. C, 24-lead ECG vest. A, mechanically induced changes in RR- and uncorrected RT-intervals at baseline and NaCl-bolus-peak in both groups, control and aLQTS (n = 13 each). B, mechanically induced changes in cardiac repolarization. Ba, illustration of average RR-corrected RTn370-intervals over time (duration of bolus injection is indicated by ‘start’ and ‘stop’) demonstrates a mechano-induced RT-prolongation (n = 13 each). Bb, box plots of baseline and peak heart rate corrected RTn370 demonstrates more pronounced RT changes in aLQTS compared to control (n = 13 each). C, example of mechanically induced changes in temporal RT-heterogeneity (STV_{RT}) in control and aLQTS (left panel: baseline; right panel: after NaCl-bolus; indicated are 15 beats before and 15 beats after peak RT). D, visualisation of mechanically induced changes in regional RT-heterogeneity (colour-coded as differences compared to minimum RT) (n = 6).

investigating MEC on the *ex vivo* whole heart level through direct control of the preload. This, in turn, should provide us with a tool for future testing of the potential role of different stretch-activated channels on mechano-electrical interactions.

Alteration of cardiac repolarization in acquired LQTS hearts *ex vivo*. The application of E-4031 (50 nM) resulted in significantly prolonged QT intervals in the *ex vivo* ECG and lengthened LV APD detected by OM (Fig. 6A & B). The RV APDs tended to increase similarly with E-4031 (Fig. 6B). However, due to pronounced motion artefacts in the RV, the APDs at RV mid could be investigated only in a subset of the hearts ($n = 2$). The physiological apico-basal difference in LV APD could be observed in control (APD75 at LV apex vs. LV mid (ms \pm SD): 115.0 ± 17.4 vs. 121.4 ± 14.6 , $P = 0.05$, $n = 6$; Fig. 6B). Interestingly, this regional heterogeneity in electrical function was not further increased in aLQTS (Δ APD75 (LV mid–LV apex) (ms \pm SD): control 6.4 ± 6.2 vs. aLQTS 6.2 ± 7.0 , $P = 0.9382$, $n = 6$).

Mechano-electrical coupling (MEC) *ex vivo*. As shown in Fig. 6Ca, unfortunately, no mechano-induced global electrical change could be detected by our model: neither

decreased (from 6 to 0 or 15 to 6 mmHg) nor increased (from 0 to 15 or 0 to 30 mmHg) preload induced any change in QT intervals at any measured time points. We could not detect any mechano-induced changes in APD (Fig. 6Cb). While mechano-induced changes in duration and/or regional heterogeneity of APD may have occurred in our model; the OM APD measurement in the beating heart was limited due to inaccuracies of the used motion tracking approach at different preloads, during which contractility and consecutive motion artefacts changed.

Discussion

In this study, we systematically assessed electro-mechanical reciprocity in healthy and E-4031-induced acquired LQTS (aLQTS) rabbit hearts to identify EMC and MEC as drivers of (potentially pro-arrhythmic) electro-mechanical heterogeneity. We confirmed previous observations on EMC in LQTS: electrical alterations (e.g. prolongation and increased dispersion of repolarisation) in aLQTS led to decreased diastolic function and prolonged contraction duration and – importantly – changed LV mechanical heterogeneity. Moreover, we demonstrated the presence of MEC in the healthy and aLQTS heart: an acute increase in mechanical preload led

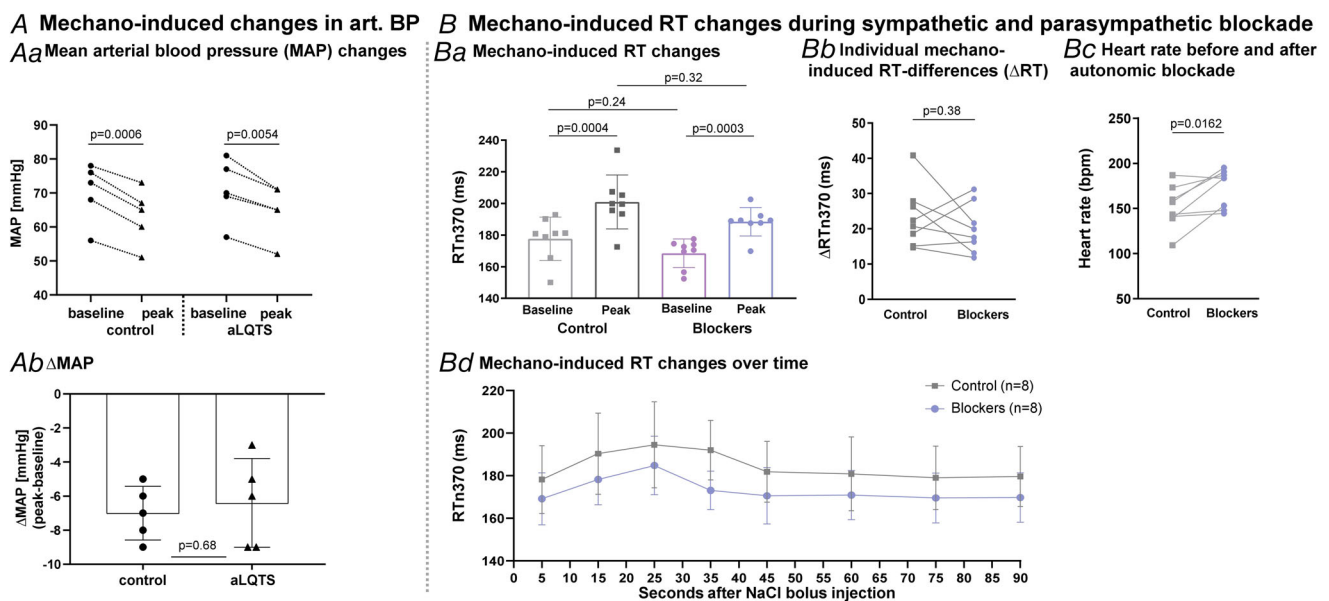


Figure 5. Mechano-induced changes in blood pressure and mechano-induced RT changes during autonomic blockade

Aa, comparison of mechano-induced changes in mean arterial blood pressure (MAP, mmHg, $n = 5$ each). Ab, comparison of delta MAP (peak-baseline) between control and aLQTS ($n = 5$ each). B, mechano-induced RT changes during sympathetic and parasympathetic blockade. Ba, mechano-induced changes in RT before (control) and after (blockers) complete blockade of the sympathetic and parasympathetic system ($n = 8$ each). Bb, comparison of mechano-induced RT changes (Delta-RT) demonstrates neither significant nor consistent differences in RT changes between baseline and blocker experiments in the individual rabbits ($n = 8$ each). Bc, comparison of heart rate before and after complete blockade of the sympathetic and parasympathetic system ($n = 8$ each). Bd, illustration of average RR-corrected RTn370-intervals over time before and after complete blockade of the sympathetic and parasympathetic system ($n = 8$ each).

to a prolongation of heart rate corrected RT-interval in both healthy and – even more – in aLQTS rabbit hearts. Additionally, we revealed a mechano-induced increase in regional RT-dispersion and alterations in the pattern of RT-heterogeneity in aLQTS.

Altered electrical heterogeneity in acquired LQTS

The measurement of electrical heterogeneity in repolarization and its deviation from a physiological magnitude is an acknowledged instrument to (indirectly) assess cardiac arrhythmogenicity (Baumert et al., 2016). We confirmed that in aLQTS rabbit hearts, short-term variability of RT (STV_{RT}), a marker for temporal heterogeneity of repolarization, as well as RT-dispersion (max-min), a marker for regional heterogeneity of repolarization, were increased significantly, which is consistent with previous findings in human subjects (Hinterseer et al., 2009; Napolitano et al., 2000). This increase in electrical heterogeneity is presumably caused by the heterogeneous distribution of the I_{Kr} conducting

hERG potassium channel. The LV apex shows a three times higher amount of hERG channel than the LV base in rabbit heart tissue (Cheng et al., 1999). As 12-lead ECG RT-dispersion only allows an assumption of changes in electrical heterogeneity but does not provide information about the actual regional differences, for example apico-basal and RV-LV heterogeneity, we designed a self-fabricated 24-lead ECG vest, enabling us to visualise acute changes in $RT_{difference}$ on the rabbits' thoraces. And indeed, using this new method, we were able to detect significant apical $RT_{difference}$ prolongation by I_{Kr} -blocker E-4031, leading to altered electrical heterogeneity in aLQTS. Also in right cardiac regions, RT-heterogeneity was altered in aLQTS compared to healthy controls. These results are in line with novel findings in ECGI, a non-invasive method depicting regional differences in the activation-recovery interval (ARI), a surrogate for APD (Vijayakumar et al., 2014), with 224-multielectrode body-surface ECG in combination with CT-based reconstruction on the human heart (Rudy, 2017; Rudy & Burnes, 1999). In ECGI, patients with congenital

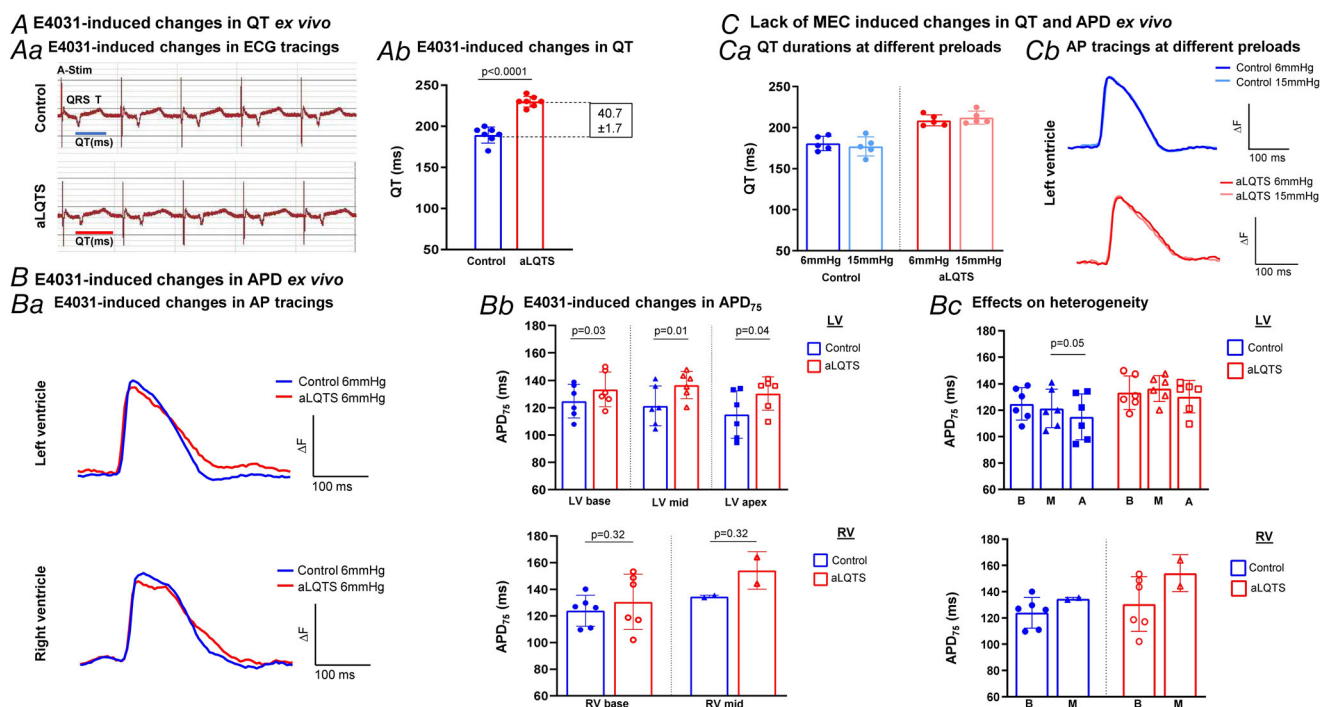


Figure 6. Ex vivo optical mapping assessment of MEC in Langendorff-perfused beating hearts

A, E-4031-induced changes in QT-intervals. Aa, original tracings of control and aLQTS ECGs during atrial stimulation (A-Stim). Indicated are QRS complex, T-wave and QT-intervals. Ab, bar graphs of E-4031 induced changes in QT. $***P < 0.001$, paired t test. B, E-4031 induced changes in APD_{75} ex vivo. Ba, representative optical AP tracings in LV and RV at baseline (control) and after E-4031 perfusion (aLQTS) are shown. ΔF = change in fluorescence intensity in arbitrary units. Bb, bar graphs of APD_{75} in LV and RV ROIs in control and aLQTS in $n = 6$ hearts (of note, for RV mid APD analyses only $n = 2$ hearts could be used due to pronounced motion artefacts in the other 4). $*P < 0.05$, paired t tests for each ROI. Bc, bar graphs of APD_{75} in LV and RV ROIs (B: base, M: mid, A: apex) in control and aLQTS visualising regional heterogeneity. $*P < 0.05$. C, lack of MEC induced changes in QT-intervals and in APD_{75} ex vivo in $n = 6$ hearts. Ca, bar graphs of QT at 6 and 15 mmHg in control and aLQTS. Cb, representative AP tracings in LV at 6 mmHg and 15 mmHg preload in control and aLQTS are shown.

LQTS type 2 (LQT2; loss-of-function mutations in *KCNH2/hERG* with reduction of I_{Kr} ; Schwartz et al., 2012) showed overall spatially heterogeneous activation-recovery intervals and steeper repolarization gradients than in healthy controls (Vijayakumar et al., 2014). Importantly ARI were strongly prolonged in RV regions in LQT2 compared to control, resulting in a much steeper gradient of repolarization across the border of LV and RV (Vijayakumar et al., 2014), similar to our vECG in aLQTS. As the acute induction of aLQTS showed comparable effects on regional repolarization pattern to genetic 'chronic' LQTS, this could either suggest that remodelling in chronic disease might be minimal, or that acute, I_{Kr} -blocker-induced electrical changes just further progress in genetic LQTS.

Altered mechanical heterogeneity in acquired LQTS

Substantiating the mounting evidence that LQTS is an 'electro-mechanical', rather than a 'purely electrical', disease, we observed impaired diastolic peak velocities (AMPdia) in the longitudinal direction (V_z) in the overall base and 4/6 mid segments and significantly prolonged *time-to-diastolic peak* duration (TTPdia), a marker for contraction duration. Moreover, we added a novel aspect to these data by revealing significant EMC-induced changes in apico-basal heterogeneity in V_z AMPdia and V_z TTPdia.

Our findings regarding the AMPdia and TTPdia are in line with our previous studies, in which longitudinal diastolic peak velocities were more affected than radial velocities in drug-induced aLQT2 (Odening et al., 2013; Ziupa et al., 2019), while in congenital LQT2 rabbit hearts longitudinal and radial velocities were similarly affected (Odening et al., 2013). The impact of E-4031 on mechanical function, however, was substantially more pronounced in our study compared to Ziupa et al.'s work in 2019 (Ziupa et al., 2019). Sex differences in the rabbits' cohorts might be the possible explanation. While Ziupa et al. examined exclusively male animals (Ziupa et al., 2019), we investigated a sex-mixed cohort, mainly consisting of female rabbits. Testosterone is known to increase I_{Kr} and I_{Ks} , making male hearts less prone to I_{Kr} -blocker-induced or congenital QT prolongation than female hearts (reviewed in Odening & Koren, 2014). In transgenic LQT2 rabbits, Lang, Menza et al. (2016) observed that female animals exhibit a prolonged TTPdia compared to males, indicating that the impact of I_{Kr} -blocker E-4031 on mechanics might be similarly more pronounced in female rabbits, leading to a potentially higher pro-arrhythmic risk in female subjects due to more prominent electrical *and* mechanical changes in aLQTS.

Accordingly, we revealed pronounced alterations of mechanical dispersion in aLQTS with decreased

apico-basal heterogeneity in diastolic peak velocities and increased apico-basal heterogeneity in contraction duration. Similarly to our findings, Brado et al. (2017) described an altered apico-basal longitudinal relaxation sequence in pediatric patients with genetic LQTS in TPM-MRI. In tissue Doppler (Borowiec et al., 2020; Haugaa, Amlie, et al., 2010) and strain (Haugaa, Edvardsen, et al., 2009; ter Bekke et al., 2015) echocardiography, comparable alterations in mechanical function have been observed in LQTS. Transmural and apico-basal alteration in mechanical relaxation, prolonged contraction duration and the so-called electro-mechanical window negativity (ter Bekke et al., 2015) – describing the abnormal closure of the aortic valve before the end of the prolonged electrical repolarization – have been reported. Importantly, regional differences in mechanical dysfunction have been linked to arrhythmic risk, with longer apical radial strain in symptomatic than in asymptomatic LQTS patients (Borowiec et al., 2020), underlining the importance of a better understanding of mechanical heterogeneity in aLQTS-related arrhythmogenesis.

Mechano-electrical coupling in healthy and aLQTS rabbit hearts

Mechanically induced changes in electrical function occur frequently, both in healthy and diseased hearts, for example due to volume or pressure overload (Quinn & Kohl, 2021), the Valsalva manoeuvre (Taggart et al., 1992), local endocardial contact caused by intracardiac devices such as catheters (Befeler, 1978; Quinn & Kohl, 2021) or due to extra-thoracic applied forces, such as *commotio cordis* (Quinn & Kohl, 2021).

In this study, we revealed a prolongation of repolarization duration (heart rate corrected RTn370-intervals) upon an increase in preload in healthy and aLQTS hearts. Importantly, these mechano-induced electrical changes, for example RT prolongation and increased heterogeneity, were particularly pronounced in aLQTS with already pre-existing prolongation of cardiac repolarization, suggesting that these hearts may be particularly prone to MEC.

Mechanically induced electrical changes are timing dependent (Quinn & Kohl, 2021); for example, they can lead to APD prolongation or shortening depending on the occurrence in relation to the cardiac cycle, and may, under physiological conditions, be part of regional synchronization of ventricular repolarization (Opthof et al., 2015; Quinn & Kohl, 2021). Over the entire cardiac cycle, the increase in mechanical preload can affect APD, ventricular refractoriness and conduction (Quinn & Kohl, 2021). In our study, we recorded a significant prolongation in cardiac repolarization in healthy and aLQTS hearts consistently around 20 s after the i.v.

bolus. This prolongation occurred to a similar extent with intact autonomic activity and after pharmacological blockade of both the sympathetic and parasympathetic nervous system, suggesting that this mechano-induced electrical alteration is not solely due to autonomic modulation/reflex loops, but may indeed be caused by cardiac-intrinsic mechanisms such as electrical alterations caused by bolus-induced changes in myocardial stretch, or a combination of both.

Of note, considering that xylazine increases the parasympathetic tone, our anaesthetic regimen might not be ideal in the setting of investigating the effect of pharmacological autonomic blockade on MEC. However, as we are interested in changes in cardiac repolarization, and it is shown that the ketamine/xylazine combination has no effect on cardiac repolarizing ion currents (Odening et al., 2008), it is an advantage to utilise this regimen as opposed to the alternative options such as propofol or isoflurane, which do block various repolarizing ion channels.

Importantly, the mechano-induced electrical alterations were particularly pronounced in aLQTS, in which not only an overall RT prolongation occurred, but also an increase in regional RT-dispersion in 12-lead ECG and a changed pattern of RT heterogeneity. These data indicate that acute changes in (global) myocardial stretch may cause additional alterations of electrical function in aLQTS. When these changes exert regionally divergent effects – as observed in our study in aLQTS – they may potentially increase proarrhythmic APD heterogeneity and thereby facilitate arrhythmia formation in acquired QT-prolongation. However, no direct evidence was provided in our rabbit model on whether these alterations in the electrical function can further evolve into arrhythmias. There are several reasons that may account for the lack of arrhythmic events in our acute drug-induced LQTS model. Not only is the I_{Kr} -blocker E-4031 a short acting drug, but we also monitored the rabbits for a short period of time and only performed one single change in preload during 12-lead ECG and one during vECG in each aLQTS animal, which might be too little to observe ME-induced arrhythmic events. Moreover, the rabbits are also under anaesthesia with ketamine/xylazine during the ME interventions, which may further contribute to a lack of arrhythmic events due to an overall relatively low sympathetic tone with parasympathetic predominance.

Along the lines of the concept of a 'sensitized' cardiac tissue in LQTS due to the disproportional prolongation of cardiac repolarization compared to the less pronounced prolongation of contraction duration (Odening et al., 2022), for example, the negative electro-mechanical window (ter Bekke et al., 2015), our findings indicate that cardiac repolarization in aLQTS may be more susceptible to acute MEC effects than healthy hearts. These effects are

likely to be exaggerated with rapid mechanical alterations, particularly if the mechanical alterations occur in the later phase of the electromechanical window, in which mechanical systole is already completed, while the electrical repolarization is still ongoing (Odening et al., 2022).

Whether this apparently increased mechano-sensitivity in LQTS is mainly because a longer cardiac repolarization is in general more prone to additional QT-prolongations – the paradigm of an 'intrinsic' APD-dependence of APD-modulation (Winter & Shattock, 2016; Zaza, 2016) – or whether the LQTS/aLQTS heart has an intrinsically increased mechano-sensitivity remains to be investigated.

The molecular mechanism behind MEC is postulated to be based on an interplay between intracellular Ca^{2+} -concentration and -sensitivity, and mechano-sensitive channels (MSCs) (Quinn & Kohl, 2021). MSCs are a group of channels that can either be directly activated by stretch (stretch-activated channels, SACs) or channels that are mainly voltage- or ligand-gated but exhibit a certain degree of mechano-sensitivity (e.g. I_{CaL} , I_{Ks} , I_{Na} und I_{KATP}) (Sachs, 2009). While non-selective SACs (SAC_{NS}) can cause depolarization and excitation in resting cells, they can accelerate early repolarization and APD-shortening during the plateau phase or prolong APD when activated later during repolarization (Quinn & Kohl, 2021). Therefore, SAC_{NS} could explain most of the observed mechano-induced electrical alterations; but it remains to be demonstrated whether these channels are the main determinant of MEC in the whole heart (Quinn & Kohl, 2021).

To provide a framework, in which the potential impact of different SACs as mediators of mechano-induced RT/APD prolongation could be investigated in the future, we aimed to establish an OM setup with a beating rabbit heart, in which the preload can be changed and resulting changes in global and regional APD can be measured. We developed the above described Langendorff-perfused 'working-heart-like' OM setup and could identify E-4031-induced APD-prolongation in beating hearts at the physiological 6 mmHg preload using our motion-correction tool. We were, however, facing several problems in accurately determining APD when increasing preload, which resulted in stronger contraction. The motion tracking approach could correct for in-plane motion, particularly in the centre of the field-of-view, but out-of-plane motion (i.e. towards or away from the camera) could not be corrected for and caused significant artefacts in the recorded signals. This precluded any consistent assessment of potential APD-changes with changed preload. However, even in the *ex vivo* surface ECG, no RT-changes were observed with changed preloads, suggesting also that the method of setting different preloads might need further improvement.

Several technical limitations of our current OM 'pseudo-beating-heart-like' setup could be improved in the future. (1) Changing to a 4-view configuration would allow better surface tracking (due to higher overlap of the different cardiac views), better motion correction, and thereby, less disturbed 'corrected' voltage-signals. (2) Adding telecentric illumination to reduce changes in light intensity with distance to the LED would improve signal quality with out-of-plane motion. (3) Taking advantage of ratiometric potentiometric dyes would further reduce motion artefacts. (4) Implementing a more physiological 'working-heart' model would enable better control of preload and could result in more physiological mechanical function. (5) Placing a second balloon into the RV would reduce rotational motion and would represent a more physiological setting, in which the preload of both ventricles could be changed and both, simultaneous preload-changes as well as acute RV-LV heterogeneities in preload could be investigated. We are currently implementing these modifications, with the aim of obtaining more accurate and regionally detailed AP signals. This will hopefully allow us to detect more subtle MEC-induced changes in APD and its heterogeneity, as well as to test the impact of activation and/or blockade of various SAC on MEC.

Conclusion

We observed mechano-induced prolongation of cardiac repolarization both in healthy and aLQTS rabbit hearts. Importantly, this mechano-induced prolongation and increased heterogeneity in repolarization was more pronounced in the aLQTS setting, suggesting that acute MEC effects may play an additional role in LQT-related arrhythmogenesis. Further mechanistic studies are needed to fully understand the extent of MEC in aLQTS and the underlying drivers. To this end, a further optimization of the panoramic 'beating-heart' OM system introduced here and the approach to implementing preload changes is warranted.

References

- Antzelevitch, C., & Fish, J. (2001). Electrical heterogeneity within the ventricular wall. *Basic Research in Cardiology*, **96**(6), 517–527.
- Baumert, M., Porta, A., Vos, M. A., Malik, M., Couderc, J.-P., Laguna, P., Piccirillo, G., Smith, G. L., Tereshchenko, L. G., & Volders, P. G. A. (2016). QT interval variability in body surface ECG: Measurement, physiological basis, and clinical value: Position statement and consensus guidance endorsed by the European Heart Rhythm Association jointly with the ESC Working Group on Cardiac Cellular Electrophysiology. *Europace*, **18**(6), 925–944.
- Befeler, B. (1978). Mechanical stimulation of the heart: Its therapeutic value in tachyarrhythmias. *Chest*, **73**(6), 832–838.
- ter Bekke, R. M. A., Haugaa, K. H., van den Wijngaard, A., Bos, J. M., Ackerman, M. J., Edvardsen, T., & Volders, P. G. A. (2015). Electromechanical window negativity in genotyped long-QT syndrome patients: Relation to arrhythmia risk. *European Heart Journal*, **36**(3), 179–186.
- Borowiec, K., Kowalski, M., Kumor, M., Duliban, J., Śmigielski, W., Hoffman, P., & Biernacka, E. K. (2020). Prolonged left ventricular contraction duration in apical segments as a marker of arrhythmic risk in patients with long QT syndrome. *EP Europace*, **22**(8), 1279–1286.
- Brado, J., Dechant, M. J., Menza, M., Komancsek, A., Lang, C. N., Bugger, H., Foell, D., Jung, B. A., Stiller, B., Bode, C., & Odening, K. E. (2017). Phase-contrast magnet resonance imaging reveals regional, transmural, and base-to-apex dispersion of mechanical dysfunction in patients with long QT syndrome. *Heart Rhythm*, **14**(9), 1388–1397.
- Brunner, M., Peng, X., Liu, G. X., Ren, X. Q., Ziv, O., Choi, B. R., Mathur, R., Hajjiri, M., Odening, K. E., Steinberg, E., Folco, E. J., Pringa, E., Centracchio, J., Macharzina, R. R., Donahay, T., Schofield, L., Rana, N., Kirk, M., Mitchell, G. F., ... Koren, G. (2008). Mechanisms of cardiac arrhythmias and sudden death in transgenic rabbits with long QT syndrome. *Journal of Clinical Investigation*, **118**(6), 2246–59.
- Cerqueira, M. D., Weissman, N. J., Dilszian, V., Jacobs, A. K., Kaul, S., Laskey, W. K., Pennell, D. J., Rumberger, J. A., Ryan, T., & Verani, M. S. (2002). Standardized myocardial segmentation and nomenclature for tomographic imaging of the heart. *Circulation*, **105**(4), 539–42.
- Cheng, J., Kamiya, K., Liu, W., Tsuji, Y., Toyama, J., & Kodama, I. (1999). Heterogeneous distribution of the two components of delayed rectifier K⁺ current: A potential mechanism of the proarrhythmic effects of methanesulfonanilideclass III agents. *Cardiovascular Research*, **43**(1), 135–147.
- HajiRassouliha, A., Taberner, A. J., Nash, M. P., & Nielsen, P. M. F. (2017). Motion correction using subpixel image registration. *Reconstruction, segmentation, and analysis of medical images* (pp. 14–23). Springer International Publishing.
- HajiRassouliha, A., Taberner, A. J., Nash, M. P., & Nielsen, P. M. F. (2018). Subpixel phase-based image registration using Savitzky–Golay differentiators in gradient-correlation. *Computer Vision and Image Understanding*, **170**, 28–39.
- Haugaa, K. H., Edvardsen, T., Leren, T. P., Gran, J. M., Smiseth, O. A., & Amlie, J. P. (2009). Left ventricular mechanical dispersion by tissue Doppler imaging: A novel approach for identifying high-risk individuals with long QT syndrome. *European Heart Journal*, **30**(3), 330–337.
- Haugaa, K. H., Amlie, J. P., Berge, K. E., Leren, T. P., Smiseth, O. A., & Edvardsen, T. (2010). Transmural differences in myocardial contraction in Long-QT syndrome. *Circulation*, **122**(14), 1355–1363.

- Hintenseer, M., Beckmann, B. M., Thomsen, M. B., Pfeufer, A., Dalla Pozza, R., Loeff, M., Netz, H., Steinbeck, G., Vos, M. A., & Kääh, S. (2009). Relation of increased short-term variability of QT interval to congenital long-QT syndrome. *American Journal of Cardiology*, **103**(9), 1244–1248.
- Hornyik, T., Castiglione, A., Franke, G., Perez-Feliz, S., Major, P., Hiripi, L., Koren, G., Bószé, Z., Varró, A., Zehender, M., Brunner, M., Bode, C., Baczkó, I., & Odening, K. E. (2020). Transgenic LQT2, LQT5, and LQT2-5 rabbit models with decreased repolarisation reserve for prediction of drug-induced ventricular arrhythmias. *British Journal of Pharmacology*, **177**(16), 3744–3759.
- Janse, M. J., Coronel, R., Opthof, T., Sosunov, E. A., Anyukhovsky, E. P., & Rosen, M. R. (2012). Repolarization gradients in the intact heart: Transmural or apico-basal? *Progress in Biophysics and Molecular Biology*, **109**(1–2), 6–15.
- Jung, B. A., Odening, K. E., Dall'Armellina, E., Föll, D., & Schneider, J. E. (2012). A comprehensive quantitative comparison of myocardial motion in mice, rabbits and humans using phase contrast MRI. *Journal of Cardiovascular Magnetic Resonance*, **14**(S1), P54.
- Lang, C. N., Koren, G., & Odening, K. E. (2016). Transgenic rabbit models to investigate the cardiac ion channel disease long QT syndrome. *Progress in Biophysics and Molecular Biology*, **121**(2), 142–156.
- Lang, C. N., Menza, M., Jochem, S., Franke, G., Perez Feliz, S., Brunner, M., Koren, G., Zehender, M., Bugger, H., Jung, B. A., Foell, D., Bode, C., & Odening, K. E. (2016). Electro-mechanical dysfunction in long QT syndrome: Role for arrhythmogenic risk prediction and modulation by sex and sex hormones. *Progress in Biophysics and Molecular Biology*, **120**(1–3), 255–269.
- Moss, R., Wülfers, E. M., Lewetag, R., Hornyik, T., Perez-Feliz, S., Strohbach, T., Menza, M., Krafft, A., Odening, K. E., & Seemann, G. (2022). A computational model of rabbit geometry and ECG: Optimizing ventricular activation sequence and APD distribution. *PLoS ONE*, **17**(6), e0270559.
- Nador, F., Beria, G., De Ferrari, G. M., Stramba-Badiale, M., Locati, E. H., Lotto, A., & Schwartz, P. J. (1991). Unsuspected echocardiographic abnormality in the long QT syndrome. Diagnostic, prognostic, and pathogenetic implications. *Circulation*, **84**(4), 1530–1542.
- Napolitano, C., Priori, S. G., & Schwartz, P. J. (2000). Significance of QT dispersion in the long QT syndrome. *Progress in Cardiovascular Diseases*, **42**(5), 345–350.
- Nerbonne, J. M. (2000). Molecular basis of functional voltage-gated K⁺ channel diversity in the mammalian myocardium. *The Journal of Physiology*, **525**(2), 285–298.
- Odening, K. E., Hyder, O., Chaves, L., Schofield, L., Brunner, M., Kirk, M., Zehender, M., Peng, X., & Koren, G. (2008). Pharmacogenomics of anesthetic drugs in transgenic LQT1 and LQT2 rabbits reveal genotype-specific differential effects on cardiac repolarization. *American Journal of Physiology Heart and Circulatory Physiology*, **295**(6), H2264–H2272.
- Odening, K. E., Jung, B. A., Lang, C. N., Cabrera Lozoya, R., Ziupa, D., Menza, M., Relan, J., Franke, G., Perez Feliz, S., Koren, G., Zehender, M., Bode, C., Brunner, M., Sermesant, M., & Föll, D. (2013). Spatial correlation of action potential duration and diastolic dysfunction in transgenic and drug-induced LQT2 rabbits. *Heart Rhythm*, **10**(10), 1533–1541.
- Odening, K. E., & Koren, G. (2014). How do sex hormones modify arrhythmogenesis in long QT syndrome? Sex hormone effects on arrhythmogenic substrate and triggered activity. *Heart Rhythm*, **11**(11), 2107–2115.
- Odening, K. E., van der Linde, H. J., Ackerman, M. J., Volders, P. G. A., & ter Bekke, R. M. A. (2022). Electromechanical reciprocity and arrhythmogenesis in long-QT syndrome and beyond. *European Heart Journal*, **43**(32), 3018–3028.
- Pilia, N., Nagel, C., Lenis, G., Becker, S., Dössel, O., & Loewe, A. (2021). ECGdeli - An open source ECG delineation toolbox for MATLAB. *SoftwareX*, **13**, 100639.
- Quinn, T. A., & Kohl, P. (2016). Rabbit models of cardiac mechano-electric and mechano-mechanical coupling. *Progress in Biophysics and Molecular Biology*, **121**(2), 110–122.
- Quinn, T. A., & Kohl, P. (2021). Cardiac Mechano-electric coupling: Acute effects of mechanical stimulation on heart rate and rhythm. *Physiological Reviews*, **101**(1), 37–92.
- Roden, D. M. (2004). Drug-induced prolongation of the QT interval. *The New England Journal of Medicine*, **350**(10), 1013–1022.
- Roden, D. M. (2008). Long-QT syndrome. *New England Journal of Medicine*, **358**(2), 169–176.
- Rudy, Y. (2017). Noninvasive ECG imaging (ECGI): Mapping the arrhythmic substrate of the human heart. *International Journal of Cardiology*, **237**, 13–14.
- Rudy, Y., & Burnes, J. E. (1999). Noninvasive Electrocardiographic Imaging. *Annals of Noninvasive Electrocardiology*, **4**(3), 340–359.
- Sachs, F. (2009). Stretch-activated ion channels: What are they? *Physiology (Bethesda, Md)*, **25**(1), 50–6.
- Schwartz, P. J., MD, L. C., & Insolia, R. (2012). Long QT syndrome: From genetics to management. *Circulation: Arrhythmia and Electrophysiology*, **5**(4), 868–877.
- Solovyova, O., Katsnelson, L. B., Kohl, P., Panfilov, A. V., Tsaturyan, A. K., & Tsyvian, P. B. (2016). Mechano-electric heterogeneity of the myocardium as a paradigm of its function. *Progress in Biophysics and Molecular Biology*, **120**(1–3), 249–254.
- Taggart, P., Sutton, P., John, R., Lab, M., & Swanton, H. (1992). Monophasic action potential recordings during acute changes in ventricular loading induced by the Valsalva manoeuvre. *British Heart Journal*, **67**(3), 221–229.
- Opthof, T., Meijborg, V. M. F., Belterman, C. N. W., & Coronel, R. (2015). Synchronization of repolarization by mechano-electrical coupling in the porcine heart. *Cardiovascular Research*, **108**(1), 181–187.

- Vijayakumar, R., Silva, J. N. A., Desouza, K. A., Abraham, R. L., Strom, M., Sacher, F., Van Hare, G. F., Haissaguerre, M., Roden, D. M., & Rudy, Y. (2014). Electrophysiologic substrate in congenital long QT syndrome. *Cardiovascular Research*, **108**, 181–187.
- Winter, J., & Shattock, M. J. (2016). Geometrical considerations in cardiac electrophysiology and arrhythmogenesis. *EP Europace*, **18**(3), 320–331.
- Zaza, A. (2016). Electrophysiology meets geometry. *Europace*, **18**(3), 317–317.
- Ziupa, D., Menza, M., Koppermann, S., Moss, R., Beck, J., Franke, G., Perez Feliz, S., Brunner, M., Mayer, S., Bugger, H., Koren, G., Zehender, M., Jung, B. A., Seemann, G., Foell, D., Bode, C., & Odening, K. E. (2019). Electro-mechanical (dys-)function in long QT syndrome type 1. *International Journal of Cardiology*, **274**, 144–151.

Additional information

Data availability statement

All data will be made available upon reasonable request to the corresponding author.

Competing interests

The authors declare that they have no known competing financial interests that could have appeared to influence the work reported in this paper.

Author contributions

R.D.L., S.N., N.A., T.H., M.M., S.J., T.P.W., G.S., C.M.Z.J., R.L. and K.E.O. conceived and designed the experiments. R.D.L., S.N., N.A., M.M., T.H., S.J., R.M. and S.P.F. performed the

experiments. R.D.L., S.N., N.A., T.H., S.J., N.P. and K.E.O. analysed and interpreted the data. R.D.L., S.N., N.A., T.H. and K.E.O. wrote the manuscript, with critical review by all authors (S.J., R.M., M.M., N.P., T.P.W., A.H., M.Z., G.S.). All authors approved the final version of the manuscript and agreed to be accountable for all aspects of the work. All persons designated as authors qualify for authorship, and all those who qualify for authorship are listed.

Funding

German Research Foundation (DFG) Project no. 394630089 to K.E.O. and G.S. Swiss National Science Foundation (SNF) grant 310030_197595 to K.E.O. C.M. Zgierski-Johnston is a member of SFB1425, funded by DFG – Project no. (394630089) : SFB1425 : (422681845).

Acknowledgements

Open access funding provided by Universitat Bern.

Keywords

cardiac electrophysiology, ECG imaging, electro-mechanical dysfunction, electromechanical reciprocity, I_{Kr} , long QT syndrome

Supporting information

Additional supporting information can be found online in the Supporting Information section at the end of the HTML view of the article. Supporting information files available:

Statistical Summary Document

Peer Review History